

Deterministic assessment of seismic risk in Constantine city, Northeast Algeria

Mouloud Hamidatou¹  · Badreddine Sbartai²

Received: 1 December 2015 / Accepted: 22 November 2016 / Published online: 5 December 2016
© Springer Science+Business Media Dordrecht 2016

Abstract Northern Algeria has experienced many destructive earthquakes throughout its history. The largest recent events occurred in El Asnam on October 10, 1980 (moment magnitude; $M_w = 7.3$), in Constantine on October 27, 1985 (surface-wave magnitude; $M_s = 6.0$), and in Zemmouri–Boumerdes on May 21, 2003 ($M_w = 6.8$). Because of the high population density and industrialization in these regions, the earthquakes had disastrous consequences and hence highlighted the vulnerability of Algeria to seismic events. To reduce seismic risk in Constantine, the capital city of East Algeria, we present a seismic risk scenario for this city, focusing on the vulnerability of the key historic areas of Coudia, Bellevue–Cilloc, and the Old City. This scenario allows us to assess the maximum ground acceleration using empirical attenuation laws, based on the following considerations: (a) the 1985 Constantine seismic event as an earthquake reference; (b) site effects related to regional geology; (c) damage to buildings, and (d) seismic vulnerability. This study shows the map of peak ground acceleration taking into account the effects of site lithology (Avib). We observe the strongest vibrations along the two rivers “Boumerzoug and Rhumel” and also, we note that the EC8 gives a good estimate acceleration in the image of the three studied areas (Bellevue–Cilloc, Coudia, and Old Town). By correlating with the geology, we observe an acceleration of 0.13 g in the neritic limestone of the rock (Old Town) something that fits with the value obtained 0.14 g (PGA) without taking into consideration the lithology. Moreover, according to the Algerian Earthquake Engineering Code (2003) (RPA), the Wilaya of Constantine is classified in the zone IIa (medium

✉ Mouloud Hamidatou
mouloudh83@yahoo.com

Badreddine Sbartai
bsbartai@hotmail.fr

¹ Department of Civil Engineering, University of August 20, 1955-Skikda, P. O. Box 26, 21000 Skikda, Algeria

² Department of Civil Engineering, University of Badji Mokhtar-Annaba, P. O. Box 12, 23000 Annaba, Algeria

seismicity) with an acceleration data of 0.25 g. This study integrates geographic information system (GIS) data into risk models.

Keywords Vulnerability index · Earthquake · Seismic risk · Damage · GIS · Acceleration

1 Introduction

Earthquakes are among the most deadly and destructive natural hazards. Seismic activity resulted in more than 2 million deaths during the last century and destroyed many cities (Duval 2007). Earthquake activity in North Algeria constitutes a constant threat to human life and property, causing major economic losses and disruption. The losses result from not only great earthquakes, such as the $M_s = 7.3$ El Asnam event of October 10, 1980 (Oued et al. 1981), but intermediate events such as the $M_s = 5.9$ Constantine earthquake of October 27, 1985 (Bounif et al. 1987) and the May 21, 2003, Zemmouri earthquake ($M_w = 6.8$) (Belazougui 2008; Meslem et al. 2012; Mébarki et al. 2013). Constantine city lies in the eastern Tellian Atlas Mountains, one of the most seismically active regions of Northeast Algeria. Assessments of seismic risk in Northeast Algeria are relatively new and started in the 1990. The current work consists of regional and local studies, mainly based on seismic risk assessment and seismic hazard (Mortgat and Shah 1978; Benouar 1996; Hamdache et al. 1998; Aoudia et al. 2000; Bouhadad and Laouami 2002; Boughacha et al. 2004; Pelàez et al. 2004, 2005, 2006; Harbi 2006; Laouami et al. 2006; Farsi and Belazougui 2007; Bensaïbi et al. 2007; Boukri et al. 2012a, b). Seismic risk assessment is already well established for major urban centers, but is still of great importance in risk assessment in more sparsely populated areas. For example, it is crucial to examine the potential impact of earthquakes on Constantine city because there are few connecting roads between the city and nearby centers. Accurate assessment of the seismic risk faced by urban areas is needed by public authorities and decision makers, who are responsible for regional planning and urbanization. Geotechnicians, architects, construction supervisors, and public works institutions, among others, must have a good understanding of the nature of the potential for soil liquefaction before making decisions related to development. Here, we present the results of a seismic risk scenario developed for Constantine city. For each at-risk element, the procedure consists of linking seismic vulnerability values with hazard values. Hazard is expressed in terms of maximum horizontal soil acceleration as a first step in risk analysis. Induced phenomena (liquefaction and landslides) are evaluated using soil data, expressed in terms of maximum triggering percentage of gravitational acceleration (PGA). For each of these hazards and for each element of seismic risk, we assess potential damage to structures in three homogeneous areas (Coudia, Bellevue–Ciloc, and Old Town). We then describe a procedure for the adaptation of existing seismic risk and vulnerability assessment approaches to account for local geographic and geologic features. Our input information comprises an earthquake scenario, earthquake catalogs, local geology, soil classification, geotechnical conditions, and building structural data and typology. We present results as maps, including distributions of peak ground acceleration (PGA) on bedrock and design ground acceleration (DGA), intensity (I), damage assessment (D), and coefficients of safety ($F_{S_{liq}}$, $F_{S_{lan}}$) for induced effects. These thematic maps constitute important basic information for sustainable socioeconomic development in Northeast Algeria.

2 Overview of Constantine city

2.1 Study area

Constantine, the second most important city in Algeria and the largest city in Northeast Algeria, is assumed to have a moderate seismic risk. It houses important economic, scientific, and cultural aspects of Algerian infrastructure. Constantine province occupies a central geographic location within the region (Fig. 1). The center of Constantine occupies an area of 232 km², with 448,374 inhabitants, yielding a high population density of 1936 inhabitants/km² (Boudemagh 2013). Many civilizations have influenced the development and architecture of the urban area throughout its long history, from the Phoenicians to modern times (Boussouf 2002).

2.2 Seismotectonic context of Constantine region

The Tellian Atlas (Northeast Algeria) is an active collision zone between the African and Eurasian plates that is experiencing shortening of ~5–6 mm/year (Anderson and Jackson 1987; Argus et al. 1989; DeMets et al. 1990). The present study area is located around of the Constantine city, where the regional tectonics has been studied previously (Fig. 2). The study area was settled in the post-PLY period, after emplacement of the Numidian layers (the uppermost structural layers in the mountain range). This area is bounded to the east by the Guelma basin (specifically, by the Temolouka Fault that separates the two basins), and to the north by an unconformity with the inner area of the Petite Kabylie, which

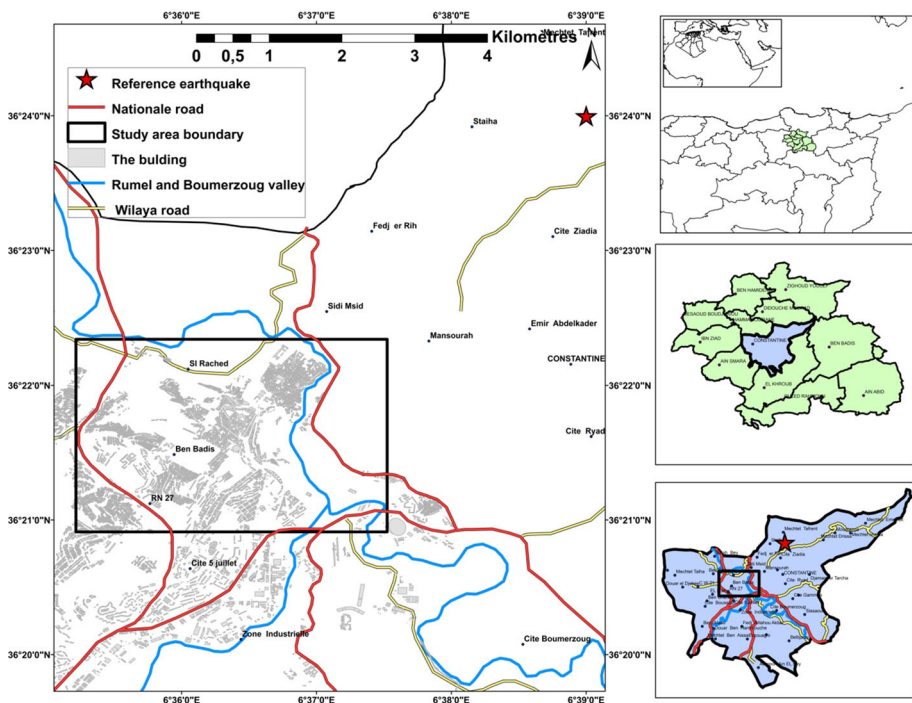


Fig. 1 Location map of Constantine city and choice reference earthquake for study area

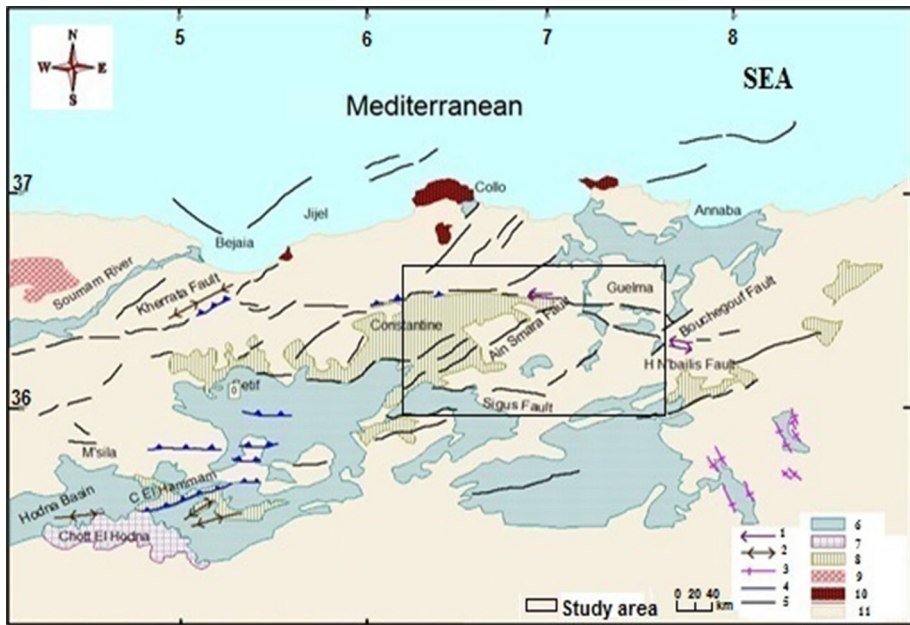


Fig. 2 Tectonic map of the study area (Constantine basin) (Harbi et al. 1999). (1) Volcanism; (2) Palcozoi; (3) Jurassic–Cretaceous and lower Cenozoic basement; (4) neogene post-nappe deposits; (5) plio-quaternary deposits; (6) quaternary deposits; (7) faults; (8) anticline; (9) reverse fault; (10) strike-slip fault; (11) normal fault

corresponds to a major structure called the Constantine North Fault (Aicha accident M'cid-Debar), oriented N100°E to N110°E (Coiffait 1992). To the south, the area is delimited by the Batna zone, where the E–W Sigus Fault marks the edge of the basin. To the west, the Setif region marks the boundary (Durand 1969; Raoult 1974; Vila 1980; Coiffait 1992; Bougdal 2007). Within this region, three important neotectonic faults cut Pliocene-Quaternary deposits. (1) The Ain Smara Fault, recognized as active since the Constantine earthquake of October 27, 1985 (Bounif et al. 1987), comprises three segments (S1, S2, and S3) extending over almost 30 km. The fault strikes NE–SW, with a dominant stress regime determined by the focal mechanism of the Constantine earthquake (Bounif et al. 1987). In this area of the Atlas Mountains, active deformation appears to be governed by transcurent dextral movement (Harbi 2001). (2) The Constantine North Fault (accident M'cid Aicha-Debar), oriented E–W and extending over 80 km, which marks the margin of the Jijel–Skikda area. (3) The Sigus Fault oriented E–W has a length of nearly 30 km.

The present study area is located in an active seismic zone within Algeria, which has been shaken by several moderate-to-strong earthquakes during the last few centuries. At least three recent earthquakes had a maximum felt intensity of at least $I_0 = \text{VII–IX}$ on the MSK scale (Bounif et al. 1987; Harbi et al. 2010), i.e., $M_s = 5.2$ on August 4, 1908, $M_s = 5.3$ on August 6, 1947, and $M_s = 5.9$ on October 27, 1985 (Ousadou et al. 2012) (Fig. 3). The inferred recurrence interval between damaging events is 39 years (Table 1). The historic seismicity of Algeria, including the Constantine region, has been studied extensively (e.g., Hée 1933, 1950; Rothé 1950; Grandjean 1954; Benhallou and Roussel 1971; Roussel 1973; Mokrane et al. 1994; Mezcua and Martinez 1983). More recently,

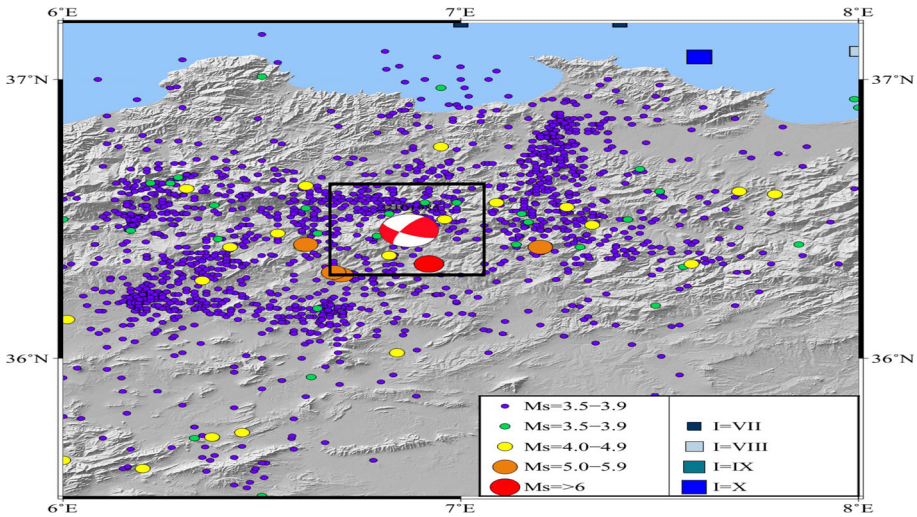


Fig. 3 Spatial distribution of earthquakes in Northeast Algeria from 1357 to 2014

Table 1 Historic seismicity in the Constantine region from Rothé (1950), Grandjean (1954). Two main historic seismic events are apparent: August 4, 1908, and August 6, 1947. The recurrence interval of the main seismic event is ~39 years

Date	Time	Location		Magnitude or intensity
		Log	Lat	
August 4, 1908	02:11	36°24'N	6°36'E	VIII Constantine
January 22, 1925	11:00	36°10'N	6°35'E	V
October 23, 1928	06:00	36°18'N	6°35'E	VI
March 19, 1946	05:23:29	36°24'N	6°36'E	(5.3) VIII–IX
August 6, 1947	09:45:38	36°18'N	6°40'E	IV
November 18, 1947	05:59	–	–	IV Constantine
December 20, 1947	10:30	–	–	IV El Khroub
July 21, 1948	11:40	–	–	IV Constantine
September 17, 1948	19:00	36°24'N	6°36'E	IV
August 25, 1959	22:31:30	36°20'N	6°40'E	V
October 27, 1985	19:34:59	36°24'N	6°39'E	(6.0) IX El Aria

reviews of historic seismicity by Harbi et al. (2003, 2010) concluded that the seismic history of the region was largely unknown before 1900 (Ousadou et al. 2012).

2.3 Creation of an earthquake scenario for the Constantine city

The Constantine city and its vicinity, with an area of about 55 km², were chosen to illustrate GIS-based risk assessment, using data on the structural vulnerabilities of different types of construction. Maps were produced from GIS databases using thematic analysis

tools in MapInfo 7.0, spatial analysis tools in ArcGIS 9.3 (Christophe 2008), and other techniques, such as georeferencing and vectorization layers (Thierno 2004). For a deterministic scenario, our choice of reference earthquake in the Constantine province was the October 27, 1985, main shock, for which the epicenter was located between El Khroub and Beni Yagoub. We used a magnitude of $M_S = 6$ and a depth of 10 km (Bounif et al. 1987). We have geologic maps (1/50,000) at this scale: the eastern part of the province, which includes the city of Constantine (Vila 1980), and the western region, which covers El Aria (Coiffait et al. 1992). The association of the two parts was used to produce a geologic map, assembled, and georeferenced (Fig. 4). We created a 1-km grid for the entire Wilaya of Constantine, a 400-m grid for the city of Constantine, a 100-m grid covering the study area, and three 20-m grids covering the buildings of the Old Town (the Rock), Coudia, and Ciloc–Bellevue (Fig. 5).

3 Methodology used for assessment of seismic risk in Constantine

The main goal of this work is to evaluate seismic risk levels for buildings and roads in the Constantine city, based on the vulnerability of infrastructure to potential seismic sources (e.g., magnitudes, distances, and source mechanisms). The methodology is based on evaluating the consequences of ground motion (PGA) for building stocks and soil (Fig. 6). Risk is assigned to each area element based on field assessments of the soil amplification coefficient (coeff) due to lithological site effects, and PGA triggering thresholds for various phenomena. Field surveys allow the assessment of ground shaking vulnerability by creating a specific vulnerability index for each building. From these, a more general vulnerability index can be developed for homogenous urban zones. PGA was computed for

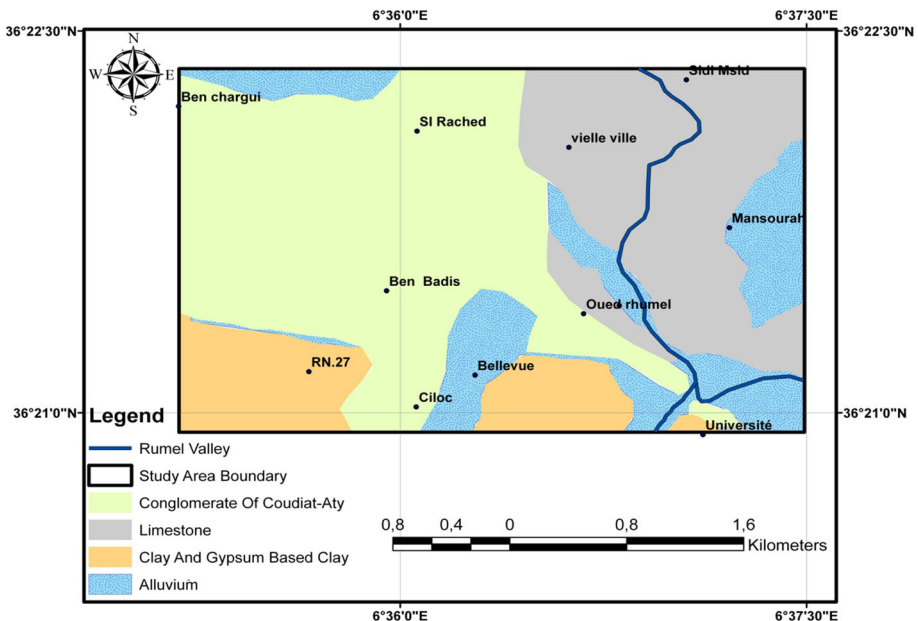


Fig. 4 Geologic map of study area

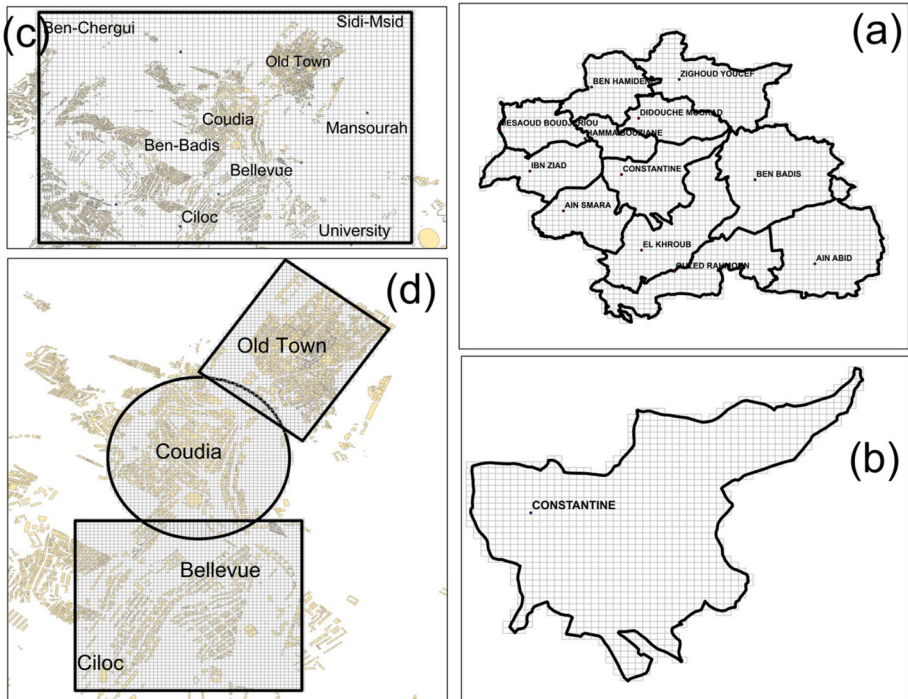


Fig. 5 Different grids: **a** grid (1 km spacing) across the Wilaya of Constantine, **b** grid (400 m) across the Constantine city, **c** grid (100 m spacing) across the study area, **d** finer grid (20 m) over Bellevue–Cilloc, Coudia, and the Old Town

the selected earthquake scenario using existing empirical attenuation laws summarized by Bommer et al. (2003). PGA values were then multiplied by site amplification factors to obtain maximum ground shaking values (A_{vib}). For each hazard phenomenon, a security factor was computed by comparing A_{vib} with a threshold T_i to estimate an event probability. Finally, a damage grade was computed by cross-referencing the vulnerability index with EMS98-intensity values derived from A_{vib} . A low-grade approach was used to infer site effect amplifications. Soil types were assigned according to building code soil classifications (NFP06-013 1995). For each soil category, an amplification factor (coeff) is given in Table 2, based on existing tables proposed for other soil classifications (TC4 2003; EC8 1998). A PGA threshold for liquefaction was assigned based on a pioneering study of susceptibility to liquefaction as a function of the age and nature of sediment deposits (Youd and Perkins 1978). Table 3 lists the PGA values corresponding to zero probability of liquefaction for each susceptibility category. These values are based on Hazus99TM (1999). The method proposed by Keefer (1984), Wilson and Keefer (1985) is used to estimate the PGA threshold for landslides (T_l). Based on the analysis of many earthquake effects, Table 4 provides the minimum PGA for triggering landslides as a function of geologic structure, slope angle, and water saturation. For each induced liquefaction and landslides, we define a security factor (F_s liq and F_s ls) to warn if a risk is likely to be triggered during an earthquake. Values of 0–1 are obtained for each factor by comparing estimated PGA (including site effects) with the threshold for a given liquefaction and landslides and site conditions (Table 5). The method used in the present study

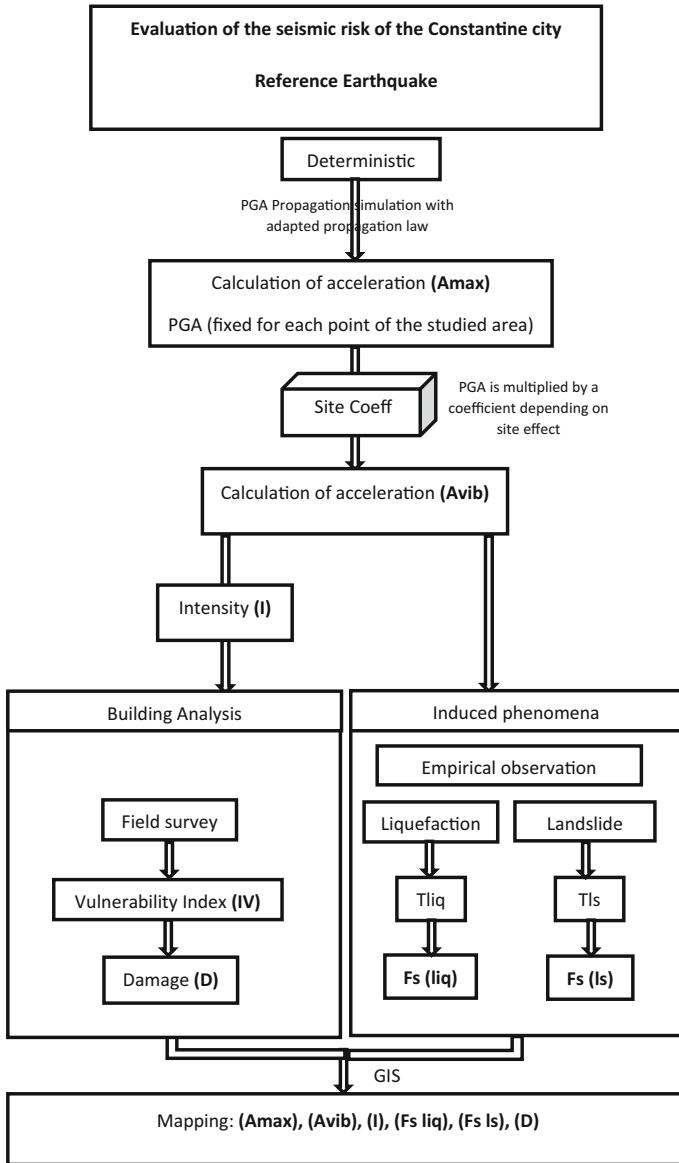


Fig. 6 Global concept of the method of the study

for the assessment of building vulnerability is derived from the European Macroseismic Scale (EMS98 1998), based on correlations between macroseismic intensity and apparent (observed) damage from past earthquakes. This vulnerability model has been improved in several studies (RADIUS, GNDT, Risk-UE, and VULNERALP) (Radius 1999; Mouroux et al. 2004; GNDT 1993a, b; Risk-UE 2003; Guéguen et al. 2007). In this work, we use a vulnerability evaluation criterion partly developed in the framework of the VULNERALP project, identical to that used by Nicem France during the GEMGEP project (Bard et al.

Table 2 Proposed amplification factors for each defined soil category (EC8 1998)

Soil type		Coeff	N SPT	Relative density (%)	Modulus (Mpa)	Vs (m/s)
Bedrock	Hard bedrock and hard chalk	1			>100	>800
Soil with good to very good geotechnical characteristics	Compact granular soil	1.35	>30	>60	>20	>400
	Soil with good coherence (clay or hard marl)				>25	
Soil with medium geotechnical characteristics	Weathered or fractured rock				50–100	300–800
	Granular soil with medium compaction	1.35	10–30	40–60	6–20	150–400
	Soil with good coherence and medium consistency + soft chalk	1.5			5–25	
Soil with weak geotechnical characteristics	Loose granular soil		<10	<40	<6	<150
	Soft coherent soil (soft clay or mud) and altered chalk	1.8	<2		<5	<150

2005). This approach, derived from that developed by the GNDT group in Italy (Benedetti and Petrini 1984; GNDT 1993b; Faccioli et al. 1999; Dolce et al. 2003), is adapted to Algerian building standards. A standardized survey and inventory form are used for data collection and the rapid determination of a vulnerability index (VI), based on building typology and aggravating factors (e.g., height, irregularities in shape, position with respect to other buildings). This makes it possible to quantitatively estimate the susceptibility to specific hazards. The vulnerability index, which ranges from zero (not vulnerable) to 100 (exceedingly vulnerable), is used to construct an empirical vulnerability (or fragility) curve for a building. This curve links a seismic event, expressed in terms of macroseismic intensity, with a damage index (*d*), from which we compute probabilities corresponding to different levels of damage. This distribution is estimated from a probability law, with parameters scaled based on actual observations of damage during various earthquakes, mainly in Italy and Greece. Using vulnerability indices obtained from field surveys makes it possible to estimate the damage rate (*d*) for a given EMS-98 intensity using the formula of Giovinazzi and Lagomarsino (2003) (Tables 6, 7). This yields a fragility function associated with each vulnerability index. The damage rate is correlated with the damage grade, defined in the EMS-98 (Table 8), but allows building distributions to be divided into five EMS-98 damage grades using a binomial formula Giovinazzi and Lagomarsino (2003).

3.1 Peak ground acceleration (PGA) on bedrock

In a deterministic scenario, the PGA of bedrock is assigned to each point in the zone. To evaluate scenarios for a particular earthquake, the user can designate an epicenter location and magnitude. Induced PGA can be computed from this information using the empirical attenuation laws of Douglas (2001). However, empirical laws are developed in local contexts and are not always generalizable. Their application, even when the conditions are fulfilled, is subject to large uncertainties that can be difficult to quantify. This must be kept

Table 3 Proposed T liquefaction (g) and PGA thresholds for landslides, as functions of geology and age. Adapted from Wilson and Keefer (1985)

Type of deposit	Proposed T_{liq} by age of deposit			
	<500 ya modern	<11 Ka Holocene	11 Ka–2 Ma Pleistocene	>2 Ma pre-Pleistocene
<i>Continental deposits</i>				
River channel	0.09	0.12	0.21	0.26
Alluvial fan and plain	0.15	0.21	0.21	0.26
Marine terrace	–	0.21	0.26	0.26
Delta and fan delta	0.12	0.15	0.21	0.26
Lacustrine	0.12	0.15	0.21	0.26
Colluvium	0.12	0.15	0.21	0.26
Dune	0.12	0.15	0.21	0.26
Loess	0.12	0.12	0.12	–
Glacial fill	0.21	0.21	0.26	0.26
Tuff	0.21	0.21	0.26	0.26
Residual soils	0.21	0.21	0.26	0.26
<i>Coastal areas</i>				
Delta	0.09	0.12	0.21	0.26
Estuarine	0.12	0.15	0.21	0.26
Beach	0.15	0.21	0.26	0.26
Lagoon	0.12	0.15	0.21	0.26
<i>Artificial embankment</i>				
Uncompact fill	0.09	–	–	–
Compacted fill	0.21	–	–	–

Table 4 Proposed T landslide (g), PGA thresholds for liquefaction (g) as a function of age, and nature of the sediment deposits. Based on Youd and Perkins (1978) and Hazus (1999)

Geologic group	Hydrological conditions	Slope angle (degrees)					
		0°–10°	10°–15°	15°–20°	20°–30°	30°–40°	>40°
Strongly cemented rocks (crystalline rocks and well-cemented sandstone, calcareous)	Wet	–	–	0.60	0.50	0.35	0.25
	Dry	–	0.4	0.25	0.20	0.15	0.15
Weakly cemented rocks and soils wet (sandy soils and poorly cemented sandstone, rock slide)	Wet	–	0.4	0.35	0.30	0.25	0.20
	Dry	0.3	0.15	0.10	0.10	0.10	0.05
Argillaceous rocks (shale, clayey wet soil, existing landslides, slump, poorly compacted fills)	Wet	0.3	0.25	0.20	0.10	0.10	0.10
	Dry	0.2	0.10	0.05	0.05	0.05	0.05

Table 5 Security factors for inducing phenomena

Fsi (security factor)	Induced phenomenon occurrence
$F_s = 0$	No release of the phenomenon
$0 < F_s \leq 0.4$	Not very probable release
$0.4 < F_s \leq 1$	Probable release
$1 < F_s \leq 2$	Nearly certain release

Table 6 Correspondence between vulnerability classes of the EMS 98 and scores of GNDT, according Giovinazzi and Lagomarsino (2003)

Method	Equivalence EMS 98—GNDT				
	A	B	C	D	E
EMS class 98					
Score GNDT	45	25	15	5	0

Table 7 Equivalence between GNDT and methods VULNERALP for environmental criteria

Environmental criteria GNDT	Materials	IV_i	Equivalence VULNERALP 1.0
Buildings on stable ground with a slope exceeding 10% The foundations are all on the same level Absence of thrust due to retaining walls	Concrete Masonry	0 0	Rock-flat terrain
Buildings on the rock with a slope of between 10 and 30% Buildings on low-quality soil with a slope of between 10 and 20%	Concrete Masonry	5 5	Rock-flat terrain Sediment-flat terrain
Height differences foundations not exceeding 1 m Absence of thrust due to retaining walls			
Buildings on the rock with a slope of between 30 and 50% Buildings on low-quality soil with a slope of between 20 and 30%	Concrete Masonry	10 25	Rock-sloped terrain Sediment-flat terrain
Height differences foundations not exceeding 1 m Absence of thrust due to retaining walls			
Buildings on the rock with a slope greater than 50% Buildings on low-quality soil with a slope greater than 30% Height differences foundations exceed 1 m Thrust due to the presence of retaining walls	Concrete Masonry	15 45	Rock-sloped terrain Sediment-sloped terrain

in mind during map analyses (Bommer et al. 2003), e.g., for laws developed from European strong motion records. For earthquakes with magnitudes $4 \leq M \leq 7.7$, epicentral distances $10 \leq D \leq 200$ km, and focal depths $Z < 30$ km, PGA is given by

$$PGA = 10^{-1.482 + 0.264M - 0.883 \log^{10} \sqrt{\left(\frac{D}{1000}\right)^2 + \left(\frac{Z}{1000}\right)^2 + 2.473^2}} \tag{1}$$

We construct a map grid where (D) is measured for each grid point.

For each mesh of the base map grid and each element of this study, the distance (D) to the earthquake is measured. The PGA is then computed from this distance (D , even if it does not fit exactly the law definition) and the magnitude (M).

Table 8 EMS-98 damage grades and corresponding damage rate ranges (EMS98 1998)

Damage grade	Damage grade level	Description	Mean damage rate, d
D0	None	No damage	0
D1	Slight	Negligible to slight damage	Inf. 0.20
D2	Moderate	Slight structural, moderate non-structural	0.21–0.40
D3	Substantial to heavy	Moderate structural, heavy non-structural	0.41–0.60
D4	Very heavy	Heavy structural, very heavy non-structural	0.61–0.80
D5	Destruction	Very heavy structural, total or near total collapse	0.81–1.00

3.2 PGA soil amplification factors (Coeff)

The aim here is to account for site effects due to soft layers above bedrock (e.g., alluvial basins), which can increase PGA and amplify damage. A low-grade approach is used. Soil type is assigned according to the French building code classification scheme (NFP06-013 1995). Based on geotechnical properties of each category, and existing tables proposed for soil classification (e.g., Borcherdt et al. 1991; TC4 2003), an amplification factor (coeff) is proposed for each soil category in Table 2. For the base map, the geologic unit crossing this study that could induce site effect is first digitalized and the most relevant coefficient of Table 2 is assigned. This step has to be clarified for this study, even if it has no influence on the resulting damage scenario map. For both base maps, the estimated PGA will be multiplied by the relative coeff to produce Avib.

3.3 PGA threshold for landslides (Tl)

Landslides are among the major consequences of earthquakes. We use the method of Keefer (1984) and Wilson and Keefer (1985) to estimate the PGA threshold for this hazard (T landslide). Table 3 gives a minimum PGA for triggering landslides as a function of deposit type and age.

3.4 PGA threshold for liquefaction (Tliq)

Liquefaction is a phenomenon that can occur when superficial sand layers lose their shear strength and act as liquids, due to rapid excitation by seismic waves. Our approach to assigning PGA liquefaction thresholds is based on the pioneering work of Youd and Perkins (1978), who investigated susceptibility as a function of age and deposit type. Table 4 shows for each of the susceptibility category, a PGA threshold corresponding to zero probability of liquefaction. These threshold values are based on Hazus99TM (1999).

3.5 PGA thresholds for induced phenomena (Ti)

To determine the soil amplification factor coeff, the PGA threshold for inducing phenomena (T_i) must be inferred from geologic maps or field surveys. For a given scenario, if $Avib > T_i$, a given phenomenon is likely to appear. The corresponding T_i value is fixed at

a very high value that cannot be realistically achieved by Avib. For both induced phenomena, we calculate a safety factor reflecting the probability that a given phenomenon occurs after the earthquake.

3.6 The method VULNERALP level 1.0

3.6.1 Vulnerability assessment

The VULNERALP method was proposed. Since some similarity exists between the Italian old buildings (especially masonry) and Algerian, it is based entirely on the method of GNDT (1993b). The weights and Italian scores of each structural criterion were considered as no return of comprehensive experience available in Algeria. However, for a context of moderate seismicity, it is essential to have a first level of evaluation (1.0 level) that is as simple as possible, for first hierarchical “seismic” buildings. That is why the structural criteria GNDT were alleviated. This implies simplified visual auscultation, especially as the GNDT was developed on the basis of observations of damage, the situation where construction is laid bare and structural criteria more easily completed. This method, certainly the most validated in Europe, also allows the representation of the damage and their equivalence to the average damage *D*, according to the European macroseismic scale (EMS98 2001) (Fig. 7). The types of constructs used in VULNERALP are identical to those detailed in EMS98. As a result, the *IV_i* function of the building material is fixed on the work presented by Giovinazzi and Lagomarsino (2003) who translated the vulnerability classes of the European Scale EMS98 in *IV_i* (Table 6).

3.6.2 Vulnerability index

The 1.0 level is established on the basis of six criteria that are structural building material, irregularity in elevation and plan, the shape of the roof, its period of construction, and the nature of the foundation within the meaning of GNDT. *IV_i* the means and the range of likely values extracted from GNDT vulnerability matrices are assigned to each criterion, for example, the GNDT four types of environment (Table 7), functions of the slope, and nature of foundation materials. These classes can be grouped in any case in rock or not, hillside or not, two levels of information that can be filled with high reliability. These two classes then have median scores and the likely intervals.







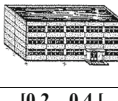


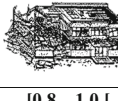
EMS98 Scale	1	2	3	4	5
Masonry structure					
Reinforced concrete structure					
Average damage	[0.0 – 0.2	[0.2 – 0.4	[0.4 – 0.6	[0.6 – 0.8	[0.8 – 1.0

Fig. 7 Equivalence between EMS98 scale damage levels and the average damage *D* calculated by the method of GNDT, according to Giovinazzi and Lagomarsino (2003)

So as to be consistent with the GNDT, structural criteria not accepted by the VULNERALP method are nevertheless taken into account in calculating the IV, the associated score (and range) corresponding to the median (and range) of values of GNDT the scores. The overall IV vulnerability index is normalized to 100. Under VULNERALP, IV_i the quality of construction is adjusted according to the time of construction, reflecting in France changing codes design and use of building materials. This strategy then connects the vulnerability to damage level compatible with that of the EMS98. Vulnerability matrices are then offered, with the range of likely values extracted from the criteria GNDT.

The overall IV of the structure is calculated by the following formula:

$$IV = \sum_{i=0}^n IV_i W_i \quad (2)$$

The average damage D is calculated based on the intensity of IEMS98 scenario earthquake and IV, and the following relationship of GNDT:

$$D = 0.5 + 0.45 \arctan(0.55(I_{EMS98} - 10.2 + 0.05IV)) \quad (3)$$

The estimated intensity for a given scenario can be mapped based on earthquake intensity using the formula of (Geoter 2002):

$$I = 3.92 \times \log_{10}(Avib) + 10.74 \quad (4)$$

Avib is a lithological term.

4 Results and discussion

In this work, we have created seismic scenarios for Constantine city, using spatial analysis with layouts suitable to determine vibrational and peak accelerations and estimate potential damage. We now present the results of our deterministic approach.

4.1 Risk assessment

Figures 8 and 9 present the peak ground acceleration values, which can reach 0.10–0.13 g for an $M = 6.0$ local earthquake. Because soil in the valley El Rhumel is mainly composed of recent quaternary alluvial deposits from the Rhumel and Boumerzoug rivers, the largest PGA values are found here. On the road between the Old Town and Boumerzoug, vibrational accelerations are estimated with soil conditions to be 0.24 g in Mansourah and Kasteur; 0.12–0.13 g in Old Town, Sidi-Msid, and Constantine University; 0.16 g in Sidi Rached and Ben Badis; and 0.20–0.22 g in Bellevue, Benchergui, Djenane-El-Zitoune, and Bent-Elisse (Fig. 10). Using geologic data, we identify homogenous zones where induced phenomena could occur. Tow threshold values corresponding to different types of induced risks are attributed to each zone. Several landslides have been detected on the slopes that border the Rhumel valley and Ciloc. Analysis of the associated slope angles, surface geologies, and hydrological conditions yields landslide threshold values of 0.10–0.25 g; the associated triggering threshold values are 0.12–0.21 g. Finally, liquefaction occurs in the main alluvial fan of the valley at 0.15 g and in secondary alluvial areas if acceleration reaches 0.09 g. The latter value may be underestimated because river alluvium is

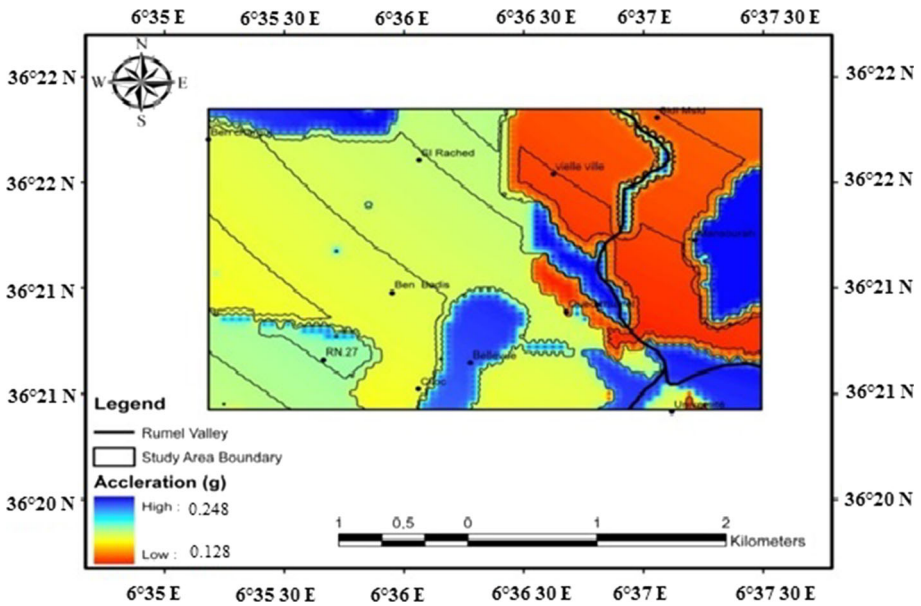


Fig. 10 Acceleration (A_{vib}) in the study area of Constantine City

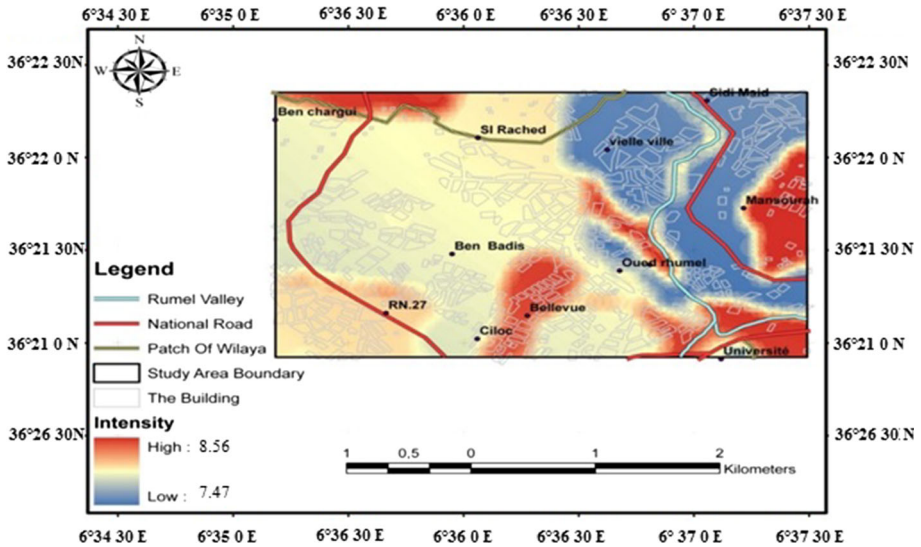


Fig. 11 Intensity (I) in the study area of Constantine City

4.2 Calculation of maximal acceleration (A_{max})

We used the attenuation law of (Bommer et al. 2003), which estimates maximum acceleration for a rocky site. The results obtained are shown in maps (Figs. 8, 9).

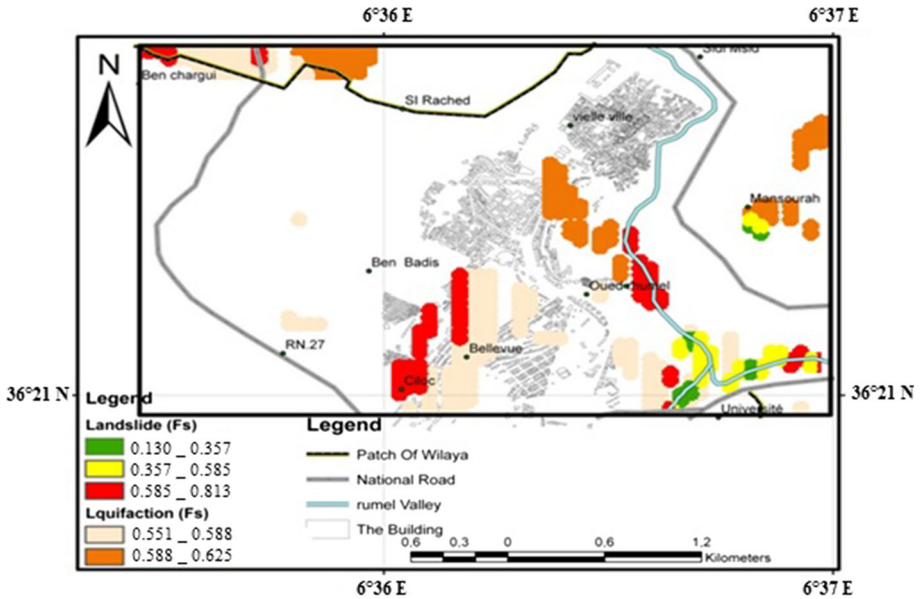


Fig. 12 Factor of safety (Fs) from the effects of the study area

4.3 Calculation of vibrational acceleration (Avib)

The same factors that amplify maximum acceleration (PGA) (e.g., lithology, EC8 1998) will change the vibration risk “Avib” significantly. The risk map in Fig. 10 shows peak ground acceleration, accounting for lithological site effects (Avib). We observe the strongest vibrations along the two rivers (Boumerzoug and Rhumel). We note that EC8 gives a good estimate of acceleration in the three study areas (Bellevue–Ciloc, Coudia, and Old Town). By integrating the acceleration with the geology, we observe an acceleration of 0.13 g in the neritic limestone (Old Town), which is similar to the value of 0.14 g (PGA) obtained without taking lithology into account. Moreover, according to the RPA (Algerian Earthquake Engineering Code), the Wilaya of Constantine is classified in Zone IIa (medium seismicity) with an expected peak acceleration rate of 0.25 g (RPA 2003).

4.4 Calculation of intensities (I)

The implementation of a damage scenario enables us to map the probable extent of damage to the Constantine city. On both maps in Fig. 10, we observe a high intensity along the two rivers (Boumerzoug and Rhumel).

4.5 Calculating the coefficients of safety (Fs) of induced effects

Figure 12 defines areas susceptible to liquefaction and landslides. From the map, we notice that liquefiable zones correspond to geologic formations (sand) in these areas, e.g., Benchergui, Bellevue, and Kef-Chadad.

4.6 Damage assessment

The use of geographic information system data has allowed us to cross-reference the vulnerability of specific neighborhoods (Bellevue–Cilloc, Coudia, and Old Town) against peak ground accelerations. Figure 13 shows estimates of damage rates for these areas: values are 0.399–0.663 for Bellevue–Cilloc, 0.501–0.738 in Coudia, and 0.634–0.793 in Old Town. We note that the highest expected rates of injury are in Old Town.

4.7 Building vulnerability estimates

Three zones were defined in Constantine city: the Coudia area, Bellevue–Cilloc, and Old Town. In all, individual vulnerabilities were assessed for 90 buildings. Old Town has the highest vulnerability index; however, indices are similar among the zones, ranging from 52 (Bellevue–Cilloc) to 69 (Old Town) (Fig. 14).

4.8 Damage evaluation

By linking PGA to the vulnerability index that we defined for the homogenous zones, we are able to estimate the mean building damage in upper Coudia. These values range between 0.502 and 0.738 (Fig. 15). Because of lithological site effects, the greatest building damage is expected in Old Town. However, only a few buildings line the Rhumel Valley; most homes are concentrated in the center of Old Town. Bellevue and Old Town are the most populated residential areas in central Constantine; it is thus interesting to study the damage that might occur at these locations on a finer scale. We find maximum damage values in the center of the Old Town. We also note that damage decreases with increasing distance from this area, reaching values as low as 0.399 (Fig. 16). Many buildings would be either destroyed or severely damaged in Old Town (Fig. 17).

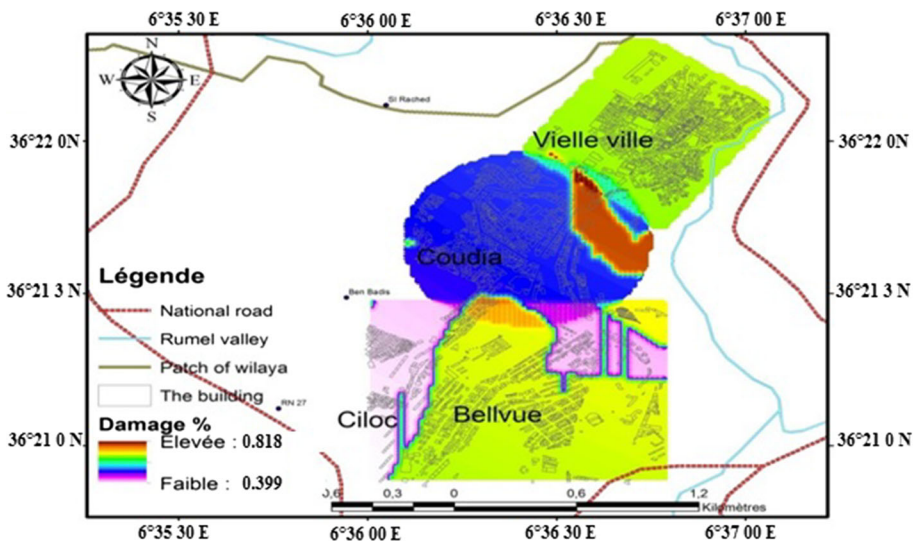


Fig. 13 Damage rates for the three districts (Bellevue–Cilloc, Coudia, and Old Town)

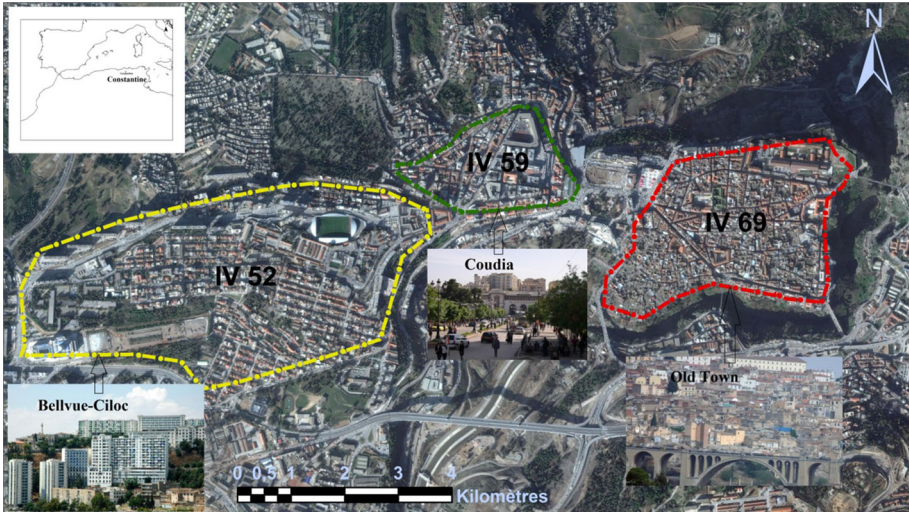


Fig. 14 Example of the boundary of the Bellevue–Cilloc area (*red-dashed line*), mean vulnerability index $IV = 52$. The boundary of the Coudia area (*green-dashed line*), mean vulnerability index $IV = 59$ and the boundary of the Old Town area (*yellow-dashed line*), mean vulnerability index $IV = 69$

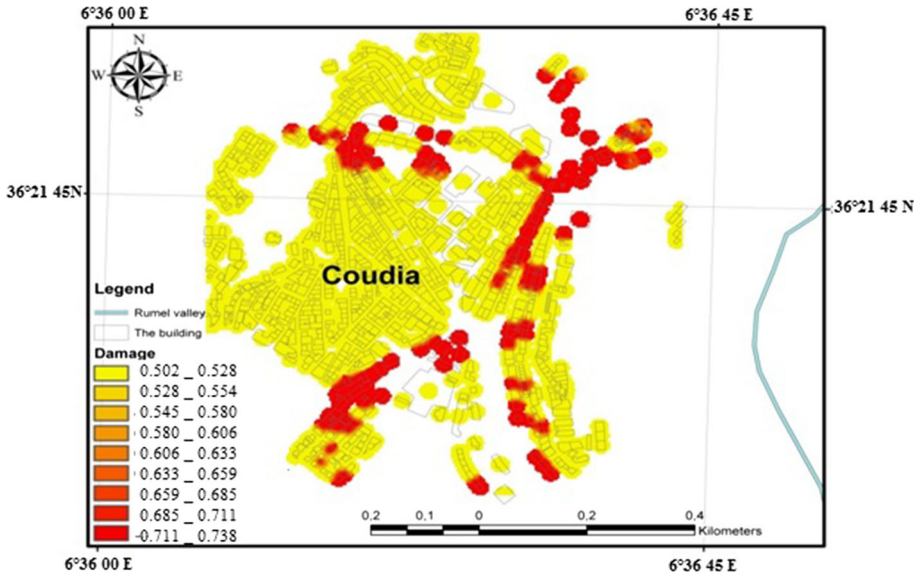


Fig. 15 Building damage Coudia square

Nevertheless, we notice that damage is more severe in Old Town than in Bellevue–Cilloc and Coudia. These increased damage levels do not solely reflect the vulnerability index, which is higher in Bellevue–Cilloc and Coudia.

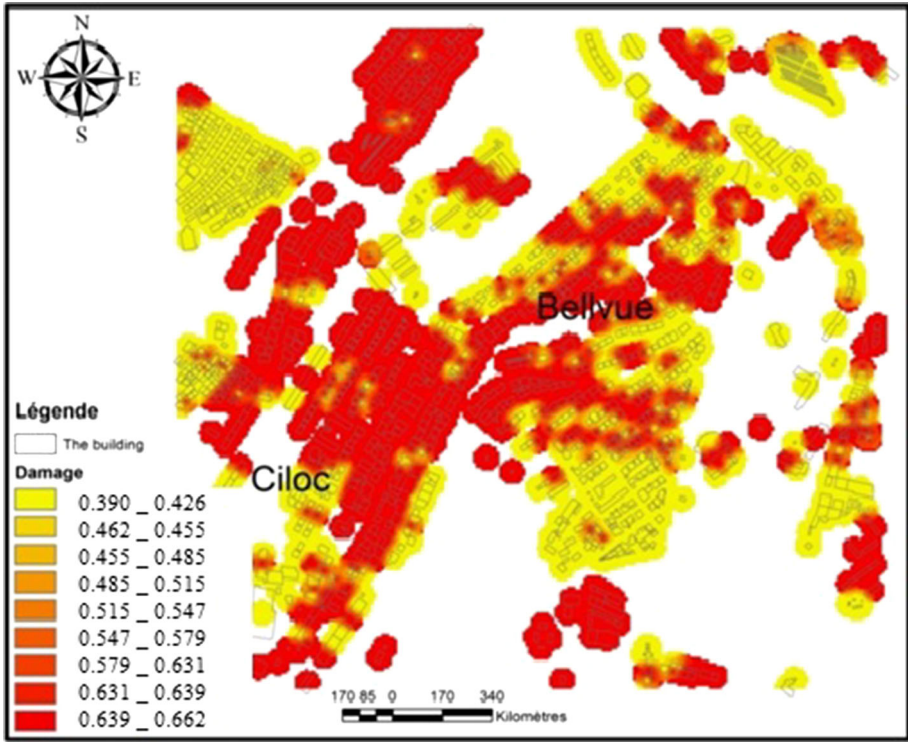


Fig. 16 Building damage Bellevue–Cilloc square

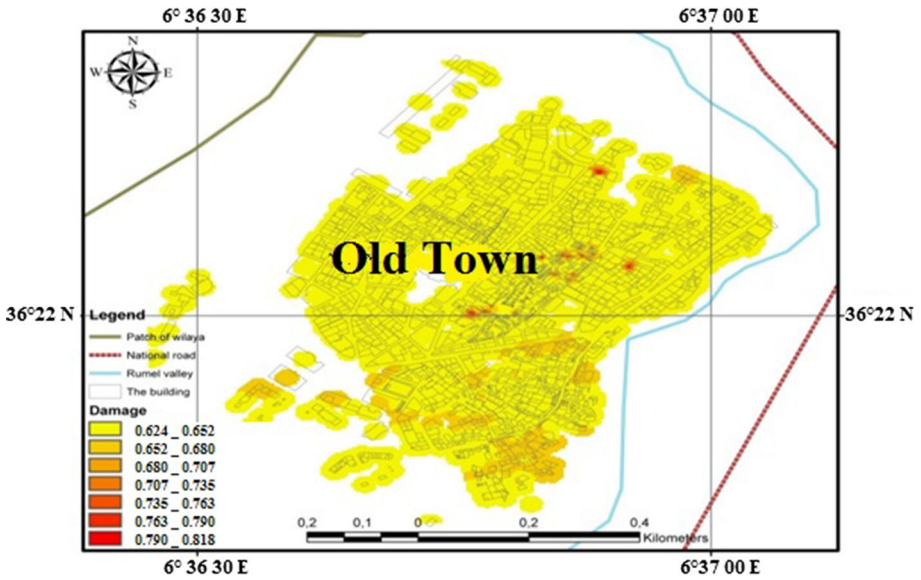


Fig. 17 Building damage Old Town square

5 Conclusions

Seismic risk assessments are priority activities in all countries that can potentially experience large earthquakes. The ultimate goal is to ensure public safety in the event of an earthquake, that is, to avoid major structural damage and loss of human lives. Damage is unavoidable but can be limited. In this work, we present a deterministic seismic risk assessment for the Constantine city, Algeria. We have assessed the seismic risk potential in detail. This work presents a methodology for assessing the likely consequences of future earthquakes in urban areas. Results are provided in the form of maps of the Constantine region. Evaluation consists of assessing the maximum acceleration of ground motion, taking site effects and area geology into account, as well as induced effects (landslides and liquefaction). Therefore, it is important that data are sufficiently well structured to be properly analyzed in GIS software, including MapInfo and ArcGIS. Of note, the direct application of EC8 yields sound estimates of alluvial PGA amplifications throughout the Constantine city. This shows that EC8 correctly accounts for lithology. Constructing such risk maps for seismically vulnerable areas permits us to (1) identify geographic areas affected by seismic risks; (2) determine more precisely whether induced effects (landslides and liquefaction) are localized on backfill, on grounds reworked by relatively old natural landslides, or on rigid bedrock affected by active deformation (e.g., seismogenic faults, broken fault, isostatic adjustment); and (3) limit the damage to buildings and to construct new buildings with seismic risk prevention in mind.

Acknowledgements The authors are grateful to the Algerian Ministry of Higher Education and Scientific Research for supporting this work. We would like to thank two anonymous reviewers for the critical reviews and useful suggestions that really improved the manuscript.

References

- Anderson H, Jackson J (1987) The deep seismicity of the Tyrrhenian sea. *Geophys J R Astron Soc* 91:613–637
- Aoudia A, Vaccari F, Suhadolc P, Meghraoui M (2000) Seismogenic potential and earthquake hazard assessment in the Tell Atlas of Algeria. *J Seismol* 4:79–98
- Argus DF, Gordon RG, De Mets C, Stein S (1989) Closure of the Africa–Eurasia–North America plate motion circuit and tectonics of the Gloria fault. *J Geophys Res* 94:5585–5602
- Bard PY, Gemgep Team (2005) Le risque sismique à Nice. Apport méthodologique, Résultats et perspectives opérationnelles. METATM, MEDD, CANCA
- Belazougui M (2008) Boumerdes Algeria earthquake of May 21, 2003: damage analysis and behavior of beam-column reinforced concrete structures. In: Proceedings of the 14th world conference on earthquake engineering, Beijing, Paper 14_01-1006
- Benedetti D, Petrini V (1984) on seismic vulnerability of masonry buildings: proposal of an evaluation procedure. *L'Ind Costr* 18:66–78
- Benhallou H, Roussel J (1971) Catalogue des Séismes Algériens de 1951 à 1970. Note I.M.P.G.A, Alger
- Benouar D (1996) Seismic hazard evaluation at Algiers using Benouar earthquake catalogue. *Nat Hazards* 13:119–131
- Bensaïbi M, Tadjer K, Brahim Mezazigh B (2007). Scénario catastrophe de la ville de Blida. In: 7th national conference AFPS Ecole Centrale Paris
- Bommer JJ, Douglas J, Strasser FO (2003) Style-of-faulting in ground motion prediction equations. *Bull Earthq Eng* 1:171–203
- Borcherdt R, Wentworth CM, Janssen A, Fumal T, Gibbs J (1991) Methodology for predictive GIS mapping of special study zones for strong ground shaking in the San Francisco bay region, CA. In: 4th int. conf. on seismic zonation, Stanford

- Boudemagh SS (2013) A City between Metamorphosis and Mutation from 19th to 21st Century. *J Civ Eng Archit* 7(3):302–309 (**Serial No. 64**)
- Bougdal R (2007) Urbanisation et mouvements de versants dans le contexte géologique et géotechnique des bassins néogènes d'Algérie du Nord. USTHB, Alger
- Boughacha MS, Ouyed M, Ayadi A, Benhallou H (2004) Seismicity and seismic hazard mapping of northern Algeria: Map of Maximum Calculated Intensities (MCI). *J Seismol* 8:1–10
- Bouhadad Y, Laouami N (2002) Earthquake hazard assessment in the oran region (Northwest Algeria). *Nat Hazards* 26:227–243
- Boukri M, Farsi MN, Belazougui M, Amellal O, Guessoum N, Mebarki A, Mezazigh B (2012a) 15 WCEE lisboa
- Boukri M, Farsi MN, Belazougui M, Amellal O, Guessoum N (2012b) Seismic risk assessment of Constantine City (Algeria). 15 WCEE lisbona
- Bounif MA, Haessler H, Meghraoui M (1987) The Constantine earthquake of October 27, 1985: surface ruptures and aftershock study. *Earth Planet Sci Lett* 85:451–460
- Boussouf R (2002) Constantine: D'une ville attractive à une ville répulsive, Laboratoire d'Aménagement du territoire. Université de Constantine, Algérie
- CGS (2003) Etude de l'aléa sismique de la région de Constantine. Rapport final du 20/11/2003
- Christophe L (2008) Points forts de ArcGIS 9.3. ESRI Géoinformatique SA
- Coiffait PhE (1992) Un bassin post-nappe dans son cadre structural: l'exemple du bassin de Constantine (Algérie nord-orientale). Thèse doctoral, Université de Nancy, p 1.442
- Coiffait B, Guellal S, Vila JM (1992) Carte géologique au 1/50.000 d'El Aria. Sonatrach. Division Hydrocarbures
- DeMets CR, Gordon G, Argus DF, Stein S (1990) Current plate motions. *Geophys J Int* 101:425–478
- Dolce M, Masi A, Marino M, Vona M (2003) Earthquake damage scenarios of the building stock of Potenza (Southern Italy) including site effects. *Bull Earthq Eng* 1:115–140
- Douglas J (2001) A comprehensive worldwide summary of strong-motion attenuation relationships for peak ground acceleration and spectral ordinates (1969 to 2000). Civil and Environmental Engineering Dept. Imperial College London, ESEE research report 01-1, p 126
- Durand DM (1969) Mise au point sur la structure du Nord-Est de la BERBERIE. *Bull Serv Carte Géol Agérie NS* 39:89–131
- Duval AM (2007) Des effets de site aux scénarios de crise sismique méthode et application. Thèse de doctorat, Ecole Nationale des Ponts et Chaussées pp 45–120
- EC-8 (1998) Design provisions for earthquake resistance of structures—part 1–1: general rules. Seismic actions and general requirements for structures. European Prestandard ENV 1998-1-1. Comité Européen de Normalisation, Brussels
- European Macroseismic Scale (1998) Conseil de l'Europe. Cahiers du centre Européen de Géodynamique et de Séismologie. Vol. 15. G. Grünthal Editor
- Faccioli E, Pessina V, Calvi GM, Borzi B (1999) A study on damage scenarios for residential buildings in Catania City. *J Seismol* 3(3):327–343
- Farsi M, Belazougui M (2007) Microzonage du risque sismique de la Wilaya d'Alger. In: 7th national conference AFPS Ecole Centrale Paris
- Geoter (2002) Révision du zonage sismique de la France, Etude probabiliste, rapport no. GTR/MATE/0701-150 synthèse, p 39
- Giovinazzi S, Lagomarsino S (2003) Seismic risk analysis: a method for the vulnerability analysis of built-up areas. In: European safety and reliability conf. ESREL, June, Maastricht
- GNDT (1993a) Manuale Per Il Rilevamento Della Vulnerabilità Sismica Degli Edifici. Gruppo Nazionale per la Difesa dai Terremoti, Rome
- GNDT (1993b) Rischio sismico di edifici pubblici—parte I: aspetti metodologici. Centro Servizi Quasco, Bologna Grünthal G (1998)
- Grandjean A (1954) Séismes d'Algérie de 1940 à 1950 inclus. *Ann. Inst. phys. Globe, Strasbourg*, 3ème partie, Géophysique, VII, 83 (Le Puy)
- Guéguen P, Michel C, Le Corre L (2007) A simplified approach for vulnerability assessment in moderate-to-low seismic hazard regions: application to Grenoble (France). *Bull Earthq Eng* 5:467–490
- Hamdache M, Bezzeghoud M, Mokrane M (1998) Estimation of seismic hazard parameters in the northern part of Algeria. *Pure Appl Geophys* 151:101–117
- Harbi A (2001) Analyse de la sismicité et mise en évidence d'accidents Actifs dans le Nord-Est Algerien. Mémoire de Magister, USTHB, Alger
- Harbi A (2006) Evaluation de l'Aléa sismique en Algérie du nord par la modélisation de l'Input sismique dans les zones urbaines et l'Établissement d'un catalogue. PhD thesis, University of Algiers

- Harbi A, Maouche S, Ayadi A (1999) Neotectonics and associate seismicity in the Eastern Tellian Atlas of Algeria. *J Seismol* 3:95–104
- Harbi A, Benouar D, Benhallou H (2003) Re-appraisal of seismicity and seismotectonics in the north-eastern Algeria part I: review of historical seismicity. *J Seismol* 1(7):115–136
- Harbi A, Peresan A, Panza G (2010) Seismicity of Eastern Algeria: a revised and extended earthquake catalogue. *Nat Hazards* 54:725–747
- Hazus (1999) Federal emergency management agency, Washington DC, Earthquake loss estimation methodology, Hazus99 (SR2). Technical manual, Chapter 4, Potential Earth Hazards
- Hée A (1933) La fréquence des tremblements de terre en Algérie, 1911–1932. *Monogr Bur Centr Seism Intern*, p 99
- Hée A (1950) Catalogue des séismes algériens de 1850 à 1911. *Ann Inst Phys Globe Strasbourg* 6:4–49
- Keefer DK (1984) Landslides caused by earthquakes. *Geol Soc Am Bull* 95:406–421
- Laouami N, Slimania A, Bouhadada Y, Chatelaina JL, Noura A (2006) Evidence for fault-related directionality and localized site effects from strong motion recordings of the 2003 Boumerdes (Algeria) earthquake: Consequences on damage distribution and the Algerian seismic code. In: *Soil dynamics and earthquake engineering* 26, pp 991–1003
- Mébariki A, Boukri M, Laribi A, Farsi MN, Belazougui M, Kharchi F (2013) Seismic vulnerability: theory and application to Algerian buildings. *J Seismol*. doi:10.1007/s10950-013-9377-0
- Meslem A, Yamazaki F, Maruyama Y, Benouar D, Kibboua A, Mehani Y (2012) The effects of building characteristics and site conditions on the damage distribution in Boumerdes after the 2003 Algeria earthquake. *Earthq Spectra* 28(1):185–216
- Mezcua J, Martínez JM (1983) Sismicidad Del Area Ibero Mogrebi. *Seccion de Sismologia*. Inst Geogr Nacional, Madrid
- Mokrane A, Ait Messaoud A, Sebai A, Ayadi A (1994) Les séismes en Algérie de 1365 a' 1992. Publication du Centre de Recherche en Astronomie, Astrophysique et Géophysique, Département: Etudes et Surveillance Sismique, ESS, CRAAG Alger-Bouzaréah, p 277
- Mortgat CP, Shah HC (1978) Seismic hazard analysis of Algeria, technical report, the John A. Blume Earthquake Engineering Center, p. 97
- Mouroux P, Bour M, Bertrand E, Le Brun B, the RISK-UE Team (2004) From geology and seismology to earthquake-risk scenarios: the RISK-UE project. In: *Proceedings of the 13th world conference on earthquake engineering*. Vancouver
- NFP06-013 (1995) Règles de construction parasismique applicables aux bâtiments, dites règles PS92, norme française, AFNOR, p 217
- Ousadou F, Dorbath L, Dorbath C, Bounif MA, Benhallou H (2012) The Constantine (Algeria) seismic sequence of 27 October 1985: a new rupture model from aftershock relocation, focal mechanisms, and stress tensors. *J Seismol*. doi:10.1007/s10950-012-9320-9
- Ouyed M, Meghraoui M, Cisternas A, Deschamps A, Dorel J, Frechet J, Gaulon R, Hatzfeld D, Philip H (1981) Seismotectonics of the E1 Asnam earthquake. *Nature* 292:26–31
- Pelàez JA, Hamdache M (2004) Comment on the paper "Earthquake hazard assessment in the oran region (Northwest Algeria)" by Youcef Bouhadada and Nasser Laouami. *Nat Hazards* 32:155–159
- Pelàez JA, Hamdache M, Pezcasado C (2005) Updating the probabilistic seismic hazard values of Northern Algeria with the 21 May 2003 $M = 6.8$ Algiers Earthquake Included. *Pure Appl Geophys* 162:2163–2177
- Pelàez JA, Hamdache M, Pezcasado C (2006) Seismic hazard in terms of spectral accelerations and uniform hazard spectra in Northern Algeria. *Pure Appl Geophys* 163:119–135
- RADIUS (1999) Risk assessment tools for diagnosis of urban areas against seismic disasters. Final Reports, United Nations Initiative towards Earthquake Safe Cities, p 37
- Raoult JF (1974) Géologie du centre de la chaîne numidique (Nord Constantinoise, Algérie). Thesis Paris Mém. Soc. Géol. Fr. 121, p 163
- RISK-UE (2003) An advanced approach to earthquake risks scenarios with to applications different European towns. WP4: Vulnerability of Current Buildings
- Rothé JP (1950) Les séismes de Kerrata et la sismicité de l'Algérie. *Bull Serv Carte Géol Alger Sér*
- Roussel J (1973) Les zones actives et la fréquence des séismes en Algérie 1716–1970. *Bull Soc Hist Natur Afrique du Nord* 64(3):11–227
- RPA (2003) Règles parasismiques algériennes (Rules of Algerian earthquake). CGS, Algeria
- TC4 (2003) Technical committee for earthquake geotechnical engineering of the international society for soil mechanics and geotechnical engineering, manual for zonation on seismic geotechnical hazards. Japanese Geotechnical Society, Dec 2003 revised 1999
- Thierno AW (2004) Initiation à Mapinfo Professional étape 1 cartographie élémentaire avec Mapinfo Professional. ENPC-LVMT, Marne-la-Vallée

Vila JM (1980) Carte géologique au 1/50.000. Thesis University of Paris VI

Wilson RC, Keefer DK (1985) Predicting aerial limits of earthquake-induced landsliding. In: J.I

Youd TL, Perkins DM (1978) Mapping of liquefaction induced ground failure potential. J GED ASCE
104(4):433–446